The dynamic mechanical behaviour of oriented ethylene–hexene-1 copolymer

J. Clements, S. A. Jawad,* G. R. Davies and I. M. Ward
Department of Physics, University of Leeds, Leeds LS2 9JT, UK

and G. Capaccio
BP Chemicals Ltd., Polymer Sciences Branch, R & D D, Sully, S. Glamorgan, CF6 2YU, UK
(Received 28 March 1984; revised 5 November 1985)

A study has been made of the structure and dynamic mechanical properties of a highly oriented ethylene–hexene-1 copolymer. Samples were prepared by tensile drawing, and by drawing followed by annealing at either constant length or unconstrained. Following previous investigations on oriented polyethylene homopolymers, the $-50°C$ plateau moduli were determined, together with estimations of the degree of crystal continuity obtained from X-ray diffraction measurements. Although general correlations were observed between the plateau moduli and the average crystal lengths, our previous intercrystalline bridge model cannot successfully model both homopolymer and copolymer data and it is concluded that for these copolymers there is a contribution to the mechanical moduli from the presence of oriented taut tie molecules as well as crystalline bridges.

(Keywords: dynamic mechanical behaviour; oriented polyethylene copolymer; X-ray diffraction)

INTRODUCTION

The morphology of highly drawn linear polyethylene (LPE) is of considerable interest, particularly in relation to the mechanical properties of such materials. In a series of recent publications from this laboratory, particular attention has been paid to the relationship between structural information derived from wide angle and small-angle X-ray scattering data and the mechanical stiffness in a non-viscoelastic regime[1-4].

In the first instance, the correlation between longitudinal crystal thickness derived from wide-angle X-ray scattering data and the $-50°C$ plateau modulus was established for a series of drawn and extruded linear polyethylenes[1,2]. Subsequently the same correlation was applied to a series of drawn and annealed samples of LPE[3,4] and was shown to be a satisfactory, even for the case of samples which exhibit 'self-hardening' after annealing and rapid quenching in the manner first described by Arridge, Barham and Keller[5].

The discovery that highly oriented ultra-high modulus products could also be obtained from ethylene–olefin copolymers[6], despite the presence of a controlled amount of short chain side branching, provided the impetus for a fresh appraisal of the relationship between structural data and mechanical stiffness. In this paper we wish to report and discuss some recent observations on the drawing and annealing of an ethylene–hexene-1 copolymer and the mechanical behaviour of the oriented materials. It has been found that in some instances the correlation between mechanical modulus and longitudinal crystal thickness is poor and some major adjustments have to be made if the correlation is to find general applicability, not only for ethylene–olefin copolymers but also for the whole range of drawn semicrystalline polymers.

* Physics Department, Science College, University of U.A.E., PO Box 15551-AL-AIN, United Arab Emirates.

EXPERIMENTAL

Sample preparation

Isotropic sheets of the copolymer Rigidex 002-55 (BP Chemicals Ltd) were prepared by compression moulding at 160°C and quenching in cold water. Oriented samples were prepared by drawing isotropic dumbbells of gauge dimensions 5×20 mm on an Instron tensile testing machine at a single temperature of 115°C. All of the samples were prepared at a drawing rate of 100 mm/min. Final draw ratios of 11, 17 and 23 were chosen.

After drawing, a further two sets of samples were made by different annealing procedures. The first set were annealed at constant length, while the second set were annealed in the absence of any external mechanical constraint. In every case the annealing was carried out in a silicone oil bath at $130.5 \pm 0.5°C$ for 15 min.

Full details and methods used for the preparation of samples have been discussed elsewhere[7-9].

Dynamic mechanical measurements

The dynamic mechanical measurements were performed at 20 Hz on samples 50 mm in length, in the temperature range $-196°C$ to $-60°C$.

The sample is subjected to a sinusoidal strain produced by a vibrator. The stress in the sample is measured by a non-bonded strain gauge transducer and the strain by a similar gauge connected to the vibrator by a calibrated spring. The storage and loss moduli were determined by comparing the relative magnitudes of the in-phase and out-

0032-3861/86/030363-06$03.00

of-phase components received by the transducers monitoring the stress and strain, respectively, using a Solartron 1172 frequency response analyser as the phase-sensitive detection system[10].

X-ray diffraction measurements

Small-angle X-ray scattering (SAXS) patterns were obtained using a Franks small angle camera attached to a Siemens microfocus X-ray tube. The scattering was recorded photographically and the long spacing L was estimated from the pattern on the film using a Joyce–Loebl microdensitometer.

Longitudinal crystal thicknesses ($\bar{L}_{002}$) were estimated from wide-angle scattering patterns using Scherrer's equation

$$\bar{L}_{002} = K\lambda/\beta\cos\theta_{002}$$

where $\bar{L}_{002}$ is the average dimension of the crystallites normal to the diffracting planes (002), β is the integral breadth of the reflection in 2θ radians, θ is the Bragg angle, λ is the wavelength and K a shape factor depending on the method of determining β. The procedures followed in the determination of $\bar{L}_{002}$ have been described in detail elsewhere[1,11].

Differential scanning calorimetry

The melting behaviour of all samples was investigated using a Perkin–Elmer DSC-2 differential scanning calorimeter (d.s.c.). Nominal heating rates of 10°C/min and 80°C/min were used.

The melting temperature T_p and the enthalpy of fusion ΔH were determined from the peak temperature and the area of the endotherm respectively. The system was calibrated using an Indium standard (melting point 156.6°C, enthalpy of fusion 6.79 cal/g).

The crystalline mass fraction (d.s.c.) was calculated from the relationship $\alpha = \Delta H/\Delta H_0$ where ΔH is the sample enthalpy of fusion and ΔH_0 is the enthalpy of fusion of a polyethylene crystal of infinite extent ($\Delta H_0 = 70$ cal/g)[12]. Note that α denotes mass fraction crystallinity and later in theoretical work χ will be used for volume fraction crystallinity.

RESULTS

Morphological changes during drawing and annealing

The longitudinal crystal thickness $\bar{L}_{002}$ (the average crystallite length along the fibre axis direction) was evaluated directly from the line broadening of the (002) wide-angle X-ray diffraction maximum using the Scherrer equation. The effects of lattice distortions on the X-ray diffraction pattern are difficult to estimate and have been ignored. The estimates of $\bar{L}_{002}$ presented in *Table 1* must therefore be considered as lower bound values only. These estimates of $\bar{L}_{002}$ are similar in kind though not in degree to those for comparable specimens of homopolymer in that there is an increase in $\bar{L}_{002}$ with increasing draw ratio and a general decrease upon annealing, although a discrimination between the two annealing procedures is observed.

The long spacing L measured directly from the small-angle X-ray diffraction patterns are presented in *Table 1*. Here again there is comparability with samples of homopolymer; that the long spacing does not change significantly for either polymer type or draw ratio is a consequence of drawing samples at the same temperature (115°C)[4,13]. The effect of annealing is significant, and the discrimination between different annealing procedures is preserved; the increase in L when samples are annealed free is more pronounced than that for samples annealed at constant length.

The results of the d.s.c. experiments performed at heating rates of 10°C/min and 80°C/min are summarised in *Table 2*. The increase in peak melting temperature T_p upon drawing at both heating rates is noticeable as is the increase in T_p with heating rate at a single draw ratio. The enthalpy of fusion ΔH shows a significant increase on drawing. The two different annealing procedures appear to have little or no significant effect on the measured values of T_p and ΔH at either heating rate, and consequently the trends observed in the as drawn samples are preserved after annealing.

Relationship between tensile modulus and drawing and annealing

The variation of the axial storage modulus, E', and the corresponding loss factor, $\tan\delta$, with temperature are shown in *Figures 1–4*, for two draw ratios (11 and 17) and a summary of the −50°C moduli is given in *Table 3*. Curves of E' against temperature for specimens of different draw ratio are similar in shape. In all cases a plateau region on the high temperature side of the γ-relaxation can be clearly seen.

Annealing always results in a substantial decrease in modulus. At both low and high draw ratio, the effect of

Table 1 Values of the longitudinal crystal thickness ($\bar{L}_{002}$) and long spacing (L) for as drawn samples (AD), samples annealed at constant length (AC) and annealed free of stress (AF). Draw ratios (λ) as indicated

λ	Treatment	$\bar{L}_{002}$ (Å)	L (Å)
11	AD	253	238
11	AC	223	289
11	AF	210	310
17	AD	290	253
17	AC	266	285
17	AF	233	311
23	AD	326	269
23	AC	308	282
23	AF	264	315

The uncertainties in the values of $\bar{L}_{002}$ and L are estimated to be ±6% and ±8%, respectively

Table 2 D.s.c. peak melting temperature T, enthalpy of fusion ΔH and crystalline mass fraction (α) of drawn copolymer. Treatments AD, AC, AF as *Table 1*. Subscripts 10 and 80 refer to heating rate used (°C/min)

λ	Treatment	T_{10} (°C)	T_{80} (°C)	ΔH_{10} (cal/g)	ΔH_{80} (cal/g)	α_{10} (%)	α_{80} (%)
11	AD	133.1	136.3	48.4	45.9	69.0	65.5
11	AC	132.2	135.3	44.4	45.6	63.4	65.1
11	AF	133.4	135.0	46.2	45.3	66.0	64.7
17	AD	138.6	142.8	51.7	53.0	73.8	75.7
17	AC	138.8	141.3	50.9	54.8	72.7	78.3
17	AF	138.6	140.3	53.6	53.7	76.5	76.7
23	AD	139.2	142.8	53.0	53.0	75.8	75.7
23	AC	139.1	143.1	52.7	55.8	75.2	79.7
23	AF	139.5	143.0	52.9	53.1	75.5	75.8

The uncertainties in the values of T are ±0.2°C at 10°C/min and ±1.2°C at 80°C/min. The uncertainties in the values of ΔH and α are ±5%

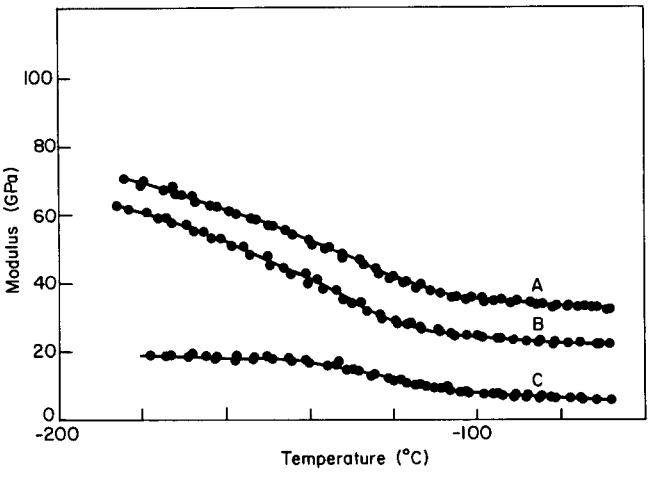

Figure 1 Axial storage modulus E' as a function of temperature for samples of draw ratio 11 (A) as drawn, (B) annealed at constant length, (C) annealed free

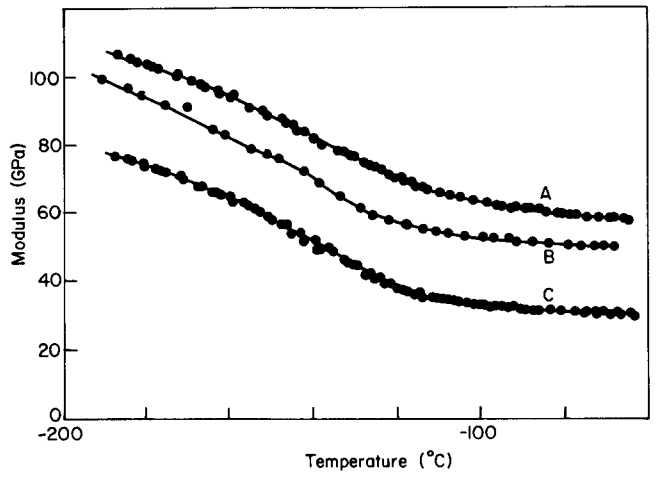

Figure 2 Axial storage modulus E' as a function of temperature for samples of draw ratio 17 (A) as drawn, (B) annealed at constant length, (C) annealed free

annealing without constraint is more pronounced than annealing with constraint. This is quite unlike the behaviour of drawn and annealed homopolymer where, at high draw ratios, the values of E' measured after the two annealing procedures are very similar over the whole temperature range[4]. The intensity of the γ relaxation, as measured by tan δ, decreases with increasing draw ratio, but increases on annealing in both cases.

DISCUSSION

The work presented here is a continuation of previous work on oriented high density polyethylene homopolymers which has resulted in a semi-quantitative understanding of the relationship between their structure and mechanical properties. Since much of the discussion of the present data relates to this earlier work we now present a summary of the previous work.

The structure of highly oriented linear polyethylene

Our previous small-angle X-ray measurements on linear polyethylene showed a two point pattern corresponding to a long period of about 200 Å. Surprisingly, however, wide-angle X-ray measurements of the integral breadth of the (002) reflection indicated an average crystal length of 300–500 Å. We therefore concluded that there was a significant fraction of crystalline chains which were longer than those in the lamellar crystals giving rise to the two point SAXS pattern. It was then postulated that these longer crystalline sequences arose from crystalline bridges between lamellar crystals, giving rise to a degree of crystal continuity which was the structural explanation for the very high moduli which were observed.

Modelling the mechanical properties

To provide a quantitative model for the mechanical modulus the crystal continuity can be treated in two alternative ways:

(1) The simplest mechanical model for such a structure is a modified Takayanagi model[1,15] where crystalline sequences linking adjacent crystal blocks are considered to act in parallel with a series combination of the remaining lamellar material and the amorphous material.

(2) Alternatively, crystalline sequences which are longer than the long period can be assumed to act like reinforcing fibres in an aligned short fibre composite whose matrix is the remaining lamellar and amorphous material[2].

It has been pointed out that the Takayanagi model and the short fibre composite model lead to similar mathematical representation for the modulus[1], although the composite model is more powerful because it can lead

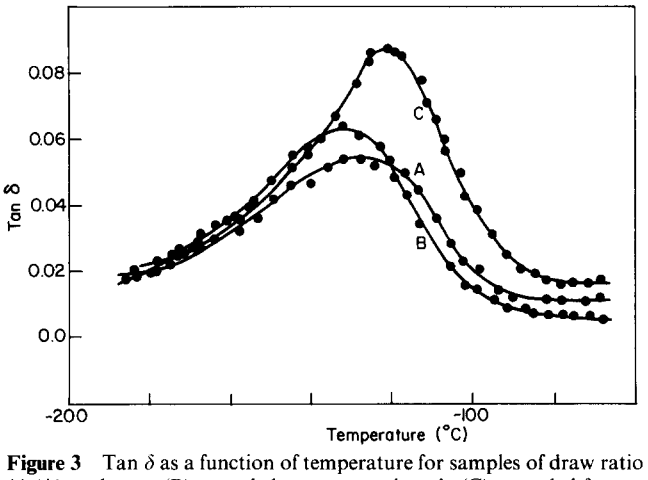

Figure 3 Tan δ as a function of temperature for samples of draw ratio 11 (A) as drawn, (B) annealed at constant length, (C) annealed free

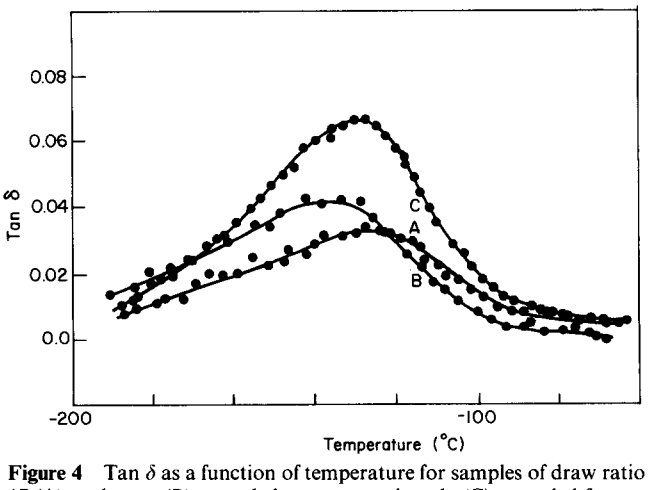

Figure 4 Tan δ as a function of temperature for samples of draw ratio 17 (A) as drawn, (B) annealed at constant length, (C) annealed free

Table 3 X-ray diffraction data and dynamic mechanical data for drawn and annealed copolymer. Treatments AD, AC and AF as *Table 1*

Draw ratio	Treatment	$\bar{L}_{002}$ (Å)	L (Å)	$\bar{L}_{002}/L$	$E'(-50°C)$ (GPa)
11	AD	253	258	0.98	31
11	AC	223	289	0.77	22
11	AF	201	310	0.65	7
17	AD	290	253	1.15	56
17	AC	266	285	0.93	49
17	AF	233	311	0.75	30
23	AD	326	269	1.21	69
23	AC	308	282	1.09	69
23	AF	264	315	0.84	37

to a more detailed understanding of the temperature dependence[16].

In both models a key factor is the fraction of crystalline sequences of length greater than the long period, and to obtain this quantity from X-ray diffraction measurements requires further assumptions. Gibson, Davies and Ward[2] postulated the following simple structural model to calculate this quantity and use it in a composite model for the mechanical properties.

Firstly, it is assumed that the SAXS long period actually reflects a repeat distance of structural and mechanical significance. Secondly, it is assumed that the distribution of crystal lengths can be calculated from a random placing of intercrystalline bridges. The degree of crystal continuity is described in terms of a single parameter p which defines the probability that an arbitrary crystal chain within a lamella traverses the disordered regions to link two adjacent lamellae. Alternatively, p represents the area fraction of intercrystalline bridge material which traverses the disordered layer. The probability f_n that a particular crystalline chain will link n lamellae is then given by

$$f_n = p^{n-1}(1-p) \tag{1}$$

since the sequence must traverse $n-1$ boundaries and fail to traverse one boundary.

The weight fraction of chains, F_n, can be obtained by multiplying f_n by the sequence length and renormalizing. If the thickness of the disordered region between lamellae is xL, where L is the small-angle long period, (see Figure 6, ref. 2), then the length of a chain linking n crystallites is $(n-x)L$, and F_n is given by:

$$F_n = \frac{(n-x)Lf_n}{\sum_{n=1}^{\infty}(n-x)Lf_n} = \frac{(n-x)p^{n-1}(1-p)^2}{1-x(1-p)} \tag{2}$$

Since the integral breadth of the 002 reflection measures a weight average chain length, then

$$\bar{L}_{002} = \sum_{n=1}^{\infty} F_n(n-x)L \tag{3}$$

The original work concentrated upon highly drawn, high crystallinity homopolymers and it was assumed that $x \ll 1$ which then gives

$$F_n = np^{n-1}(1-p)^2 \tag{4}$$

and

$$\frac{\bar{L}_{002}}{L} = \frac{1+p}{1-p} \tag{5}$$

This may be rearranged to give

$$p = \frac{\bar{L}_{002}-L}{\bar{L}_{002}+L} \tag{6}$$

This model therefore allows one to determine p from X-ray measurements. Knowing p and the volume fraction crystallinity χ one can then calculate the volume fraction V_f of crystalline sequences which link at least two lamellae:

$$V_f = \chi \sum_{n=2}^{\infty} F_n = \chi p(2-p) \tag{7}$$

As mentioned above, in a modified Takayanagi model, crystalline sequences linking two or more lamellae are assumed to act in parallel with a series combination of the remaining lamellar material and the amorphous material. If it is assumed that the modulus of the amorphous material is small compared with the crystal modulus E_c then the Young's modulus of the sample E' is given by

$$E'/E_c = V_f = \chi p(2-p) \tag{8}$$

This model has been extremely successful in describing and explaining the mechanical behaviour of highly oriented polyethylene homopolymers under a variety of conditions[2-4] using a value of 255 GPa for E_c derived from X-ray measurements[1].

The alternative short fibre composite model essentially produces a similar expression for the modulus except that the effective stiffness of the reinforcing crystals is reduced by a 'shear lag factor' ϕ so that

$$E'/E_c = \phi\chi p(2-p)$$

The inclusion of a shear lag factor allows a correlation to be made between shear and tensile data[16] over a wide temperature range but requires that a higher value of 315 GPa, derived from theoretical work[17], be used for the crystal modulus.

With the previous analysis in mind, we can now proceed to analyse the new data presented here.

Applicability of previous analysis to present data

The difference between the data now obtained and those for a drawn homopolymer (Rigidex 50) is clearly exhibited in *Figure 5* where E' ($-50°C$) is plotted as a function of $\bar{L}_{002}/L$. It is immediately obvious that, for most copolymer samples, $\bar{L}_{002}$ is less than L. This suggests no crystal continuity even though these samples have

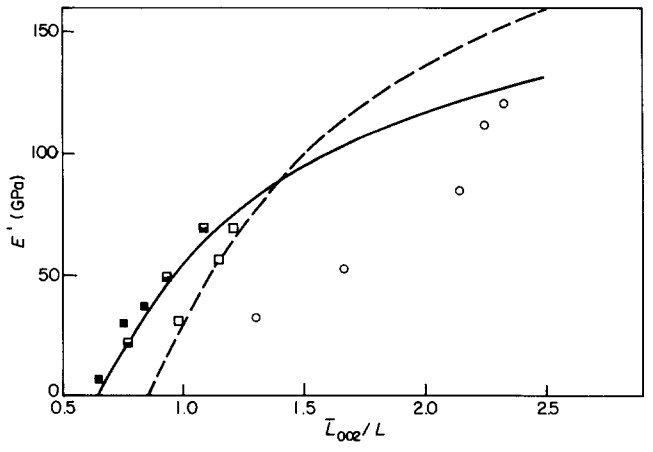

Figure 5 Axial storage modulus E' as a function of $\bar{L}_{002}/L$ (see text). Theoretical prediction: (———) $\chi=0.65$, (– – –) $\chi=0.85$. Experimental data: (○) Rigidex 50 homopolymer as drawn; (□) Rigidex 002-55 copolymer as drawn; (⬓) Rigidex 002-55 copolymer annealed at constant length; (■) Rigidex 002-55 copolymer annealed free

enhanced moduli which would suggest a significant crystal bridge content.

The first obvious step in resolving this dilemma is to continue with the full analysis from equation (3) above without assuming that $x \ll 1$. Indeed, in a simple lamellar stack model $x=(1-\chi)$ and since the copolymer samples are in general of lower crystallinity than the homopolymers the length of the intercrystalline bridges may well be longer. If we assume that x and χ are independent of draw ratio we then obtain

$$p=A(\bar{L}_{002}-AL)/(A\bar{L}_{002}+L) \tag{9}$$

where

$$A=1-x(1-p) \tag{10}$$

and

$$x=1-\chi \tag{11}$$

Since p occurs in the expression for A, these equations are best solved by a simple iterative approach which, as experience will show, rapidly converges.

It is easy to see that high values of χ (small values of x) and large values of p lead to values of A which are close to one and hence, under these conditions, equation (9) will reduce to equation (6). This was the rationale for using equation (6) in our previous studies of highly drawn homopolymers. The full analysis shows, however, that finite values of p can still occur even when $\bar{L}_{002}<L$ provided that $\bar{L}_{002}/L>\chi$. This is the case for all but the freely annealed samples and hence intercrystalline bridges could still be present in the majority of samples in the present study.

The full expression for V_f should be

$$V_f=\frac{\chi p(2-p)}{[1-(1-\chi)(1-p)^2]} \tag{12}$$

and it is this quantity (with p determined from equations (9)–(11)) which should be used in the Takayanagi or short fibre composite models.

If we determine V_f as outlined above, the only remaining parameters required are the crystallinity and crystal modulus. The crystal modulus is presumably similar for both homopolymer and copolymer so we must assign the differences in behaviour to differences in crystallinity. The solid curve in *Figure 5* represents the predictions of the Takayanagi model using a value of 255 GPa for the crystal modulus and a crystallinity of 65%. The broken curve represents the predictions of the same model for a crystallinity of 85%. This covers the maximum possible range of crystallinities and though the fit to the low draw ratio copolymer data has been improved, it can be seen that the homopolymer data is now rather poorly fitted. The fit to the homopolymer data could be improved by using the shear lag model but only at the expense of a worse fit to the copolymer data. We must therefore conclude that there are differences between the homopolymer and copolymer samples, other than simply their crystallinity which materially affect their mechanical properties.

The oriented non-crystalline phase or taut tie molecules

We must consider the possibility that other stiffening elements are present in addition to crystalline bridges. An obvious candidate is an oriented non-crystalline phase.

The small concentration of short chain butyl side branches which is present in this copolymer could conceivably hinder the development of crystalline bridges and account for the lower values of $\bar{L}_{002}$. This oriented non-crystalline phase could contribute to the plateau modulus, whilst not contributing to the average longitudinal crystal thickness. It is essentially non-crystalline and therefore has no discrete X-ray diffraction pattern. We may therefore envisage the interlamellar material in these copolymers to consist of a mixture of crystal bridges and highly oriented noncrystalline tie molecules, as proposed by Peterlin[13].

Melting point determinations have shown that the melting behaviour of drawn copolymers is similar to that of drawn homopolymers. The melting temperatures are comparable at equivalent heating rates and draw ratios, and both superheat. As we have shown previously, superheating is indicative of one or other of two morphologies: long crystals or crystals connected by taut tie molecules. Ultimately it proves difficult to distinguish between these two causes of superheating. It is therefore quite consistent to propose a structure where interlamellar material consists of both crystal bridges and taut tie molecules.

A sharp distinction between crystal bridges and taut tie molecules may be quite inappropriate. It is difficult to envisage isolated tie molecules; it seems more probable that 'bundles' of chains cross interlamellar boundaries. Crystal bridges, where they exist, are likely to have high defect concentrations, particularly in the case of copolymers where side branches will be rejected from the lamellar material and concentrate in the interlamellar material. The problem remains, however, to estimate the extent and stiffness of anything but a crystalline bridge.

The effects of annealing on the morphology and stiffness

Earlier we reported the effects of annealing on the measured values of long spacing L and longitudinal crystal thickness $\bar{L}_{002}$, and found that in every case the long period L was greater than $\bar{L}_{002}$. We then inferred, as we have done elsewhere, that these results are indicative of a conversion of the as drawn structure, where some degree

of crystal continuity exists, to a parallel lamellae texture with no crystal continuity. This conversion to a parallel lamellae texture accounts for the reduction in stiffness observed upon annealing, since the crystal continuity which we believe to be responsible for the high stiffness of as drawn material, is now absent. This applies equally to any taut tie molecules present, since they will undoubtedly relax upon annealing.

The discrimination which we observe between samples annealed at constant length and annealed freely is present in wide-angle and small-angle X-ray diffraction patterns. At both low and high draw ratio some loss of orientation is evident in WAXS patterns of samples annealed freely, while SAXS patterns display a complex 6 point pattern. In a previous publication[4] on the annealing of drawn homopolymer, we attributed these new features to melting processes during annealing followed by recrystallization on cooling; newly crystallized lamellae would not necessarily have the same high degree of orientation. We suggest that such melting and recrystallization also occur in the present series of copolymers, and that the resultant loss of orientation is primarily responsible for the lower stiffness of annealed free samples.

CONCLUSIONS

Several conclusions can be drawn from this work. Firstly, the introduction of a small, controlled amount of short chain side branching has significant effects on both physical properties and structure. Secondly, although ultra high moduli are still achievable, the correlation of moduli to structure is not as straightforward as it is for drawn homopolymers where it can be quantitatively related to the crystal continuity. Some additional factor must be included, and we consider that this additional factor is the presence of a significant concentration of 'taut' tie molecules. Although we do not have any direct experimental evidence for the existence of a distinct oriented non-crystalline phase, we conclude that the distinction between oriented non-crystalline chains and crystalline bridges is inappropriate with regard to mechanical modulus. Finally, the annealing behaviour of this copolymer is consistent with, though not identical to, the annealing behaviour of the homopolymers which we have examined.

REFERENCES

1 Clements, J., Jakeways, R. and Ward, I. M. *Polymer* 1978, **19**, 639
2 Gibson, A. G., Davies, G. R. and Ward, I. M. *Polymer* 1978, **19**, 683
3 Clements, J., Jakeways, R., Ward, I. M. and Longman, G. W. *Polymer* 1979, **20**, 295
4 Capaccio, G., Clements, J., Hine, P. J. and Ward, I. M. *J. Polym. Sci., Polym. Phys. Edn.* 1981, **19**, 1435
5 Arridge, R. G. C., Barham, P. J. and Keller, A. *J. Polym. Sci., Polym. Phys. Edn.* 1977, **15**, 389
6 Capaccio, G. and Ward, I. M. *J. Polym. Sci., Polym. Phys. Edn.* 1984, **22**, 475
7 Capaccio, G. and Ward, I. M. *Nature (Phys. Sci.)* 1973, **243**, 143; *Polymer* 1974, **15**, 233
8 Capaccio, G., Crompton, T. A. and Ward, I. M. *J. Polym. Sci., Polym. Phys. Edn.* 1976, **14**, 1641
9 Capaccio, G., Crompton, T. A. and Ward, I. M. *Polymer* 1976, **17**, 645
10 Davies, G. R., Smith, T. and Ward, I. M. *Polymer* 1980, **21**, 221
11 Clements, J. *Ph.D. Thesis*, Leeds University, 1978
12 Hamada, F., Wunderlich, B., Şumida, T., Hayashi, S. and Nakajima, A. *J. Phys. Chem.* 1968, **72**, 178
13 Peterlin, A. *J. Polym. Sci.* 1967, **C18**, 123
14 Fischer, E. W., Goddar, H. and Peisczek, W. *J. Polym. Sci.* 1971, **C32**, 149
15 Takayanagi, M., Imada, K. and Kajiyama, T. *J. Polym. Sci.* 1966, **C15**, 263
16 Gibson, A. G., Jawad, S. A., Davies, G. R. and Ward, I. M. *Polymer* 1982, **23**, 349
17 Tashiro, K., Kobayashi, M. and Tadokoro, H. *Macromolecules* 1978, **11**, 914